**Atmospheric
Chemistry
and Physics**

H_2 vertical profiles in the continental boundary layer: measurements at the Cabauw tall tower in The Netherlands

M. E. Popa[1,2]**, A. T. Vermeulen**[1]**, W. C. M. van den Bulk**[1]**, P. A. C. Jongejan**[1]**, A. M. Batenburg**[2]**, W. Zahorowski**[3]**, and T. Röckmann**[2]

[1]Energy research Centre of the Netherlands, Petten, The Netherlands
[2]Institute for Marine and Atmospheric Research Utrecht, Utrecht University, Utrecht, The Netherlands
[3]Australian Nuclear Science and Technology Organisation, Menai, New South Wales, Australia

Abstract. In-situ, quasi-continuous measurements of atmospheric hydrogen (H_2) have been performed since October 2007 at the Cabauw tall tower station in the Netherlands. Mole fractions of H_2, CO and several greenhouse gases are determined simultaneously in air sampled successively at four heights, between 20 and 200 m above ground level. ^{222}Rn measurements are performed in air sampled at 20 and 200 m.

This H_2 dataset represents the first in-situ, quasi-continuous long-term measurement series of vertical profiles of H_2 in the lower continental boundary layer. Seasonal cycles are present at all heights in both H_2 and CO, and their amplitude varies with the sampling height. The seasonality is evident in both the "baseline" values and in the short term (diurnal to synoptic time scales) variability, the latter being significantly larger during winter.

The observed H_2 short term signals and vertical gradients are in many cases well correlated to other species, especially to CO. On the other hand, H_2 has at times a unique behaviour, due to its particular distribution of sources and sinks.

Our estimation for the regional H_2 soil uptake flux, using the radon tracer method, is $(-1.89 \pm 0.26) \times 10^{-5}$ g/(m^2 h), significantly smaller than other recent results from Europe.

H_2/CO ratios of the traffic emissions computed from our data, with an average of 0.54 ± 0.07 mol:mol, are larger and more variable than estimated in some of the previous studies in Europe. This difference can be explained by a different driving regime, due to the frequent traffic jams in the influence area of Cabauw. The H_2/CO ratios of the large scale pollution events have an average of 0.36 ± 0.05 mol:mol; these ratios were observed to slightly increase with sampling height, possibly due to a stronger influence of soil uptake at the lower sampling heights.

1 Introduction

Molecular hydrogen (H_2) is an important constituent of the atmosphere, with a global tropospheric average mole fraction of about 530 parts per billion (ppb) (Novelli et al., 1999). Still atmospheric H_2 has until recently received less attention than other atmospheric components like the ozone depleting substances or the greenhouse gases.

Research on atmospheric H_2 increased since hydrogen started to be considered an important energy carrier for the future. The need to reduce emissions of pollutants and of the Kyoto regulated greenhouse gases supports the choice of hydrogen as fuel, as the burning of hydrogen produces only water. However, the total emissions of pollutants and greenhouse gases associated with the usage of H_2 depend on the method of production (e.g. using traditional fossil fuel or renewable sources of energy) and can even be larger than the emissions from direct use of fossil fuel.

Large scale usage of H_2 as fuel will most probably lead to increased H_2 emissions from leakages during production, transport and storage. On the other hand, the reduction of fossil fuel usage will lead to a decrease of the H_2 emissions associated with fossil fuel burning. It is at this moment difficult to predict whether the combination of these two factors will lead to a net increase or decrease of the total flux to the atmosphere and what the effect will be on the atmospheric budget of H_2 (Prather, 2003; Schultz et al., 2003; Tromp et al., 2003; Warwick et al., 2004). This difficulty arises partly

Correspondence to: M. E. Popa
(epopa2@yahoo.com)

from the fact that the atmospheric budget of H_2 and the processes affecting it are not well known.

Sources and sinks of atmospheric H_2 are approximately balanced in the present atmosphere. The different components of the H_2 budget have been estimated based on various approaches, initially using up-scaling from emission studies or related trace gases (e.g. CO), but recently also chemistry transport models, inverse modeling, or the use of deuterium component of H_2 (Bousquet et al., 2011; Ehhalt and Rohrer, 2009; Hauglustaine and Ehhalt, 2002; Novelli et al., 1999; Pieterse et al., 2011; Pison et al., 2009; Price et al., 2007; Rhee et al., 2006; Sanderson et al., 2003; Xiao et al., 2007; Yver et al., 2011).

Sources of atmospheric hydrogen are both natural and anthropogenic. Photochemical oxidation of methane and non-methane hydrocarbons (NMHC) is estimated to constitute about 50 % of the total H_2 source. Emissions from fossil fuel and biomass burning, both anthropogenic and natural, account for about 40 %, while volcanoes, biogenic fixation of N_2 and oceans add up to about 10 %. The main sink of H_2 is uptake by soil, estimated to account for 75 % of the total removal of hydrogen from the atmosphere. About 25 % of H_2 is lost by reaction with OH radicals, which is the reason that H_2 affects the tropospheric chemistry. As CH_4 is also consumed by reaction with OH radicals, an increase in H_2 would lead to a decrease in available OH radicals and thus to an increase in CH_4 lifetime, which makes H_2 an indirect greenhouse gas. All these global estimates have large uncertainties, and there are still significant differences between estimates based on different methods.

The global distribution of H_2 reflects the distribution of its main sink. Due to a larger land area, the mean mole fraction in Northern Hemisphere (NH) is by about 15–30 ppb lower than in the Southern Hemisphere (SH); within the NH, the H_2 mole fractions are on average larger in the tropics than at higher latitudes (Khalil and Rasmussen, 1990; Novelli et al., 1999; Price et al., 2007; Pieterse et al., 2011; Rice et al., 2010; Simmonds et al., 2000). The few studies reporting vertical distributions of H_2 from flight measurements over the northern mid-latitudes, as well as models (Price et al., 2007; Schmidt, 1978; Pieterse et al., 2011) showed increases in H_2 mole fractions with the increasing height, which is consistent with the soil being the main sink of H_2.

The mechanism of H_2 uptake by soil is not yet fully understood. Microorganisms have been shown to consume H_2 in certain conditions (e.g. Harris et al., 2007; King, 2003a, b); nonetheless it is widely considered that extracellular enzymes are the main responsible for the H_2 soil uptake (Conrad, 1995, 1996; Conrad and Seiler, 1981, 1985; Guo and Conrad, 2008; Schuler and Conrad, 1991). The uptake of H_2 by soil is temperature dependent as expected from microbial or enzymatic activity; however soil moisture was found in most cases to be the main control on the H_2 soil uptake, with an optimum around 20–30 % water holding capacity (whc) (Conrad and Seiler, 1981; Constant et al., 2008, 2009;

Gödde et al., 2000; Liebl and Seiler, 1976; Schmitt et al., 2009; Schuler and Conrad, 1991; Smith-Downey et al., 2006; Yonemura et al., 1999, 2000). At high soil moisture levels, the pores are filled with water, which reduces the soil uptake by limiting H_2 diffusion; at very low soil moisture levels, the H_2 uptake is reduced due to a reduction in the enzymatic activity (the latter situation is rarely met in field studies).

The large anthropogenic sources of H_2 are like the sinks located on land, thus largely in the NH. As the main anthropogenic sources of H_2 and CO are similar, short term increases in H_2 and CO from local sources above the non-contaminated background level are usually correlated. This provides the possibility to estimate the anthropogenic H_2 emissions, based on the better known CO fluxes (e.g. Novelli et al., 1999). A series of recent studies in Europe showed consistent results for the H_2/CO ratio of traffic emissions, of about 0.47 mol:mol (Hammer et al., 2009; Vollmer et al., 2007; Yver et al., 2009). The emissions from other anthropogenic sources are less well known and have potentially a wider range of H_2/CO ratios; moreover, due to the different effect of soil deposition on the two tracers, the integrated atmospheric signal depends on the distance from the source and is thus more difficult to interpret. Recent reported H_2/CO molar ratios for mixed anthropogenic emissions range between 0.15–0.20 at Mace Head (Grant et al., 2010b) and 0.3–0.4 at continental sites (Barnes et al., 2003; Hammer et al., 2009; Steinbacher et al., 2007).

Atmospheric measurements of H_2 were first made after 1950 (e.g. Glueckauf and Kitt, 1957; Schmidt, 1974; Scranton et al., 1980). Later, measurements at multiple locations around the globe allowed to estimate the global distribution of H_2 (Khalil and Rasmussen, 1990; Langenfelds et al., 2002; Novelli et al., 1999). Most of these measurements took place at remote locations. Long term measurements close to continental areas were first started at Mace Head, Ireland (Grant et al., 2010b; Simmonds et al., 2000), Monte Cimone, Italy (Bonasoni et al., 1997) and Harvard Forest, Massachusetts (Barnes et al., 2003).

In recent years a series of studies focused on atmospheric hydrogen in Europe, in particular on the H_2 soil sink and on emissions from anthropogenic sources, especially road traffic (Aalto et al., 2009; Bond et al., 2010; Hammer and Levin, 2009; Hammer et al., 2009; Lallo et al., 2008, 2009a, b; Schmitt et al., 2009; Steinbacher et al., 2007; Vollmer et al., 2007, 2010; Yver et al., 2009). Most of these studies were made in the framework of the EU project EuroHydros (2006–2009, Project no. 03916) which contributed to developing the measurement network in Europe and to establishing a common calibration scale for H_2 (Jordan and Steinberg, 2011).

We add to this expertise the results from a different measurement station, the tall tower Cabauw, in the Netherlands, where H_2 has been measured quasi-continuously since September 2007. Cabauw is a 200 m research dedicated tower and it is part of the European network of tall towers

for greenhouse gas measurements that was set up in the CHIOTTO project (Ref. No. EVK2-CT-2002-00163) and continued in CarboEurope IP (Ref. No. GOCE-CT-2003-505572). Since the 1990s, a new approach has been developed to measure greenhouse gases and additional tracers in the continental boundary layer using tall towers. The rationale is to measure close to continental sources and sinks, and from a sufficient height above ground that a signal which is regional to continental can be observed. The usual strategy is to measure air from several sampling heights, in order to distinguish between signals from different influence areas. Although 15–20 such tall atmospheric measurement towers exist worldwide (9 of them in Europe), Cabauw is to our knowledge the only tall tower performing continuous in-situ H_2 measurements.

This paper presents the first three years of H_2 vertical profiles measurements at Cabauw, constituting the first long term measurement series of H_2 vertical profiles in the lower troposphere. We first describe the technical setup and the quality check procedures and results. We illustrate the main characteristics of the observed signals, including interesting features of the vertical gradients. In the last part of the paper, we investigate the soil sink fluxes in the area, and the H_2/CO ratios of typical pollution signals.

2 Methods

2.1 Site description

The measurement station Cabauw (station code: CBW) is a 213 m tall tower located in the centre of the Netherlands (Lat: 51°58′ N, Long: 4°55′ E, Alt: −2 m a.s.l.), which was specifically built for meteorological research. The tower is owned by KNMI (Royal Netherlands Meteorological Institute) and hosts various collaborative measurements of meteorological parameters, pollutants, aerosols, clouds and trace gases under the name of CESAR (Cabauw Experimental Site for Atmospheric Research).

The area surrounding Cabauw tower is dominated by grassland and agricultural terrain, as can be seen in Fig. 1. In the immediate vicinity of the tower the terrain is open pasture. The North Sea is about 50 km to the WNW, and important urban areas, like Utrecht, Rotterdam and Amsterdam, are located within few tens of kilometres. The population density in the area is relatively high, about 300/km² in the surrounding 10 km, and about 900/km² in the surrounding 50 km. Besides high population density, the Netherlands has also the most dense motorway network in the European Union (57.5 km road per 1000 km²). The soil in the tower surroundings consists of 0.6 m of river-clay, overlying a thick layer of peat. The water table is about 1 m below the surface, but can be higher during wet periods.

As shown by Henne et al. (2010) the influence area (footprint) of the Cabauw tower is much wider than of most continental stations, due in principle to the high wind speeds; a detailed discussion on the representativity and footprint of Cabauw can be found in Vermeulen et al. (2011).

Greenhouse gas measurements were first started at Cabauw in 1992 as part of National Research Projects on Climate Change (Vermeulen et al., 1999) and were extended in 2004, within the EU-funded project CHIOTTO. The measurement system in operation since 2004 was designed to measure in-situ, quasi-continuously, mole fractions of CO_2, CH_4, CO, N_2O and SF_6 in air sampled at four heights of the tower (20, 60, 120 and 200 m). The setup includes a LiCor-7000 non-dispersive infrared analyzer (NDIR) for CO_2, and an Agilent 6890N gas chromatograph (GC) with a flame ionization detector (FID) and an electron capture detector (ECD) for CH_4, CO, N_2O and SF_6.

A reduction gas analyzer (RGA) for H_2 measurements was integrated into the existing measurement system in September 2007, additionally providing a second set of CO data. The setup of the RGA measurement and the data acquired during the first three years of operation constitute the subject of this paper. The setup and results of the other measurements at Cabauw are presented in Vermeulen et al. (2011).

Supporting ^{222}Rn measurements are performed in air sampled at two heights of the tower, 20 and 200 m. Measurements of various meteorological parameters are provided by KNMI (http://www.cesar-database.nl/).

2.2 Instrumental setup

A simplified diagram of the trace gas measurement system is shown in Fig. 2. Atmospheric air is continuously drawn from 4 heights of the tower (20 m, 60 m, 120 m, 200 m a.g.l.) via Dekabon® 12 mm OD tubing at a flow rate of 12–15 l/min. Nafion™ membrane dryers (Perma Pure LLC) are installed at the air intakes for a first drying stage. The measurement laboratory is situated at the base of the tower. Here, a 400 ml/min stream is separated from the air bulk (the rest is flushed outside) and driven through custom made glass traps immersed in a cryogenic bath where the air is dried to a dewpoint of about −50 °C (Neubert et al., 2004). The sample air is further divided, one part being directed to the CO_2 analyzer (150 ml/min), and other (80 ml/min) to the GC and RGA instruments which are installed in series.

H_2 and CO are measured with an RGA-3 reduction gas analyzer (Trace Analytical Inc.), using Helium as a carrier gas. The sample loop has a volume of 5 ml and it is temperature stabilized. The sample air is first separated inside a Molsieve-5A packed chromatographic column maintained at 110 °C. The sample is then carried over a heated bed of mercuric oxide (HgO), where the reducing compounds CO and H_2 react with the HgO. The reaction results mercury vapour, which is detected by UV absorption, and the signal is proportional to the H_2 or CO concentration in the sample air.
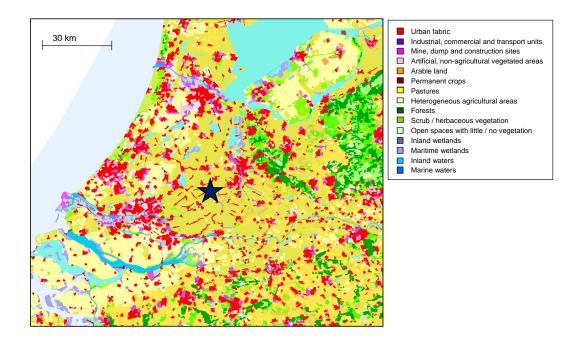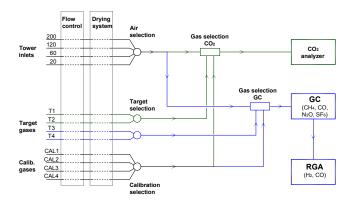
Fig. 1. Corine land cover 2000 (CLC2000) map around the Cabauw tall tower station. The star shows the location of the Cabauw tower.

The daily calibration is made using a set of four aluminium high pressure cylinders (Luxfer model P2806Z, volume 50 l, maximum working pressure 200 bar) with Rotarex-Ceodeux valves (model D20030163, brass, with PCTFE seat) and Scott regulators (model 51-14C, high purity, two stages, Ni platted brass, SS diaphragm). The cylinders have been filled with atmospheric air and calibrated at the Max Planck Institute for Biogeochemistry Jena, Germany (MPI-BGC). The assigned H_2 values have been updated to the new hydrogen calibration scale MPI-2009 (Jordan and Steinberg, 2011), and the CO values are linked to NOAA 2000 scale.

The initial set of calibration cylinders had a H_2 mole fraction range between 146 ppb and 540 ppb, covering only partly the range of atmospheric variability (as it will be seen in Sect. 4.1). A new calibration gas with a H_2 mole fraction of about 845 ppb was brought in use in August 2009, and the remaining three calibration gases were replaced by new ones in April 2010; the present calibration scale covers the range 320–845 ppb.

The system includes four additional high pressure cylinders filled at ECN laboratory with normal atmospheric air (T1... T4 in Fig. 2). Only two of these cylinders (T3 and T4) are dedicated to the GC and RGA measurement. These two cylinders are measured half-hourly and their use is as follows. One of them (either T3 or T4) is used during the calculation of the mole fractions, to correct for variations of instrument sensitivity; this cylinder is referred to as "Working Tank", or WT. The remaining cylinder is not involved in the calculation of mole fractions, but used as independent means for quality check. This cylinder is referred to as "Target Tank", or TT.

Fig. 2. Principle (simplified) scheme of the trace gases measurement system at Cabauw.

The same sample (air or gas) is measured by the three analyzers (CO_2 analyzer, GC and RGA). One measurement takes 5 min, dictated by the duration of the GC analysis. During the default measurement sequence, the atmospheric air from the four heights of the tower is measured successively, followed by two cylinder measurements (T3 and T4). In this way a vertical profile is determined every half hour. The daily calibration sequence consists of measuring once each of the four calibration gases, also followed by the two cylinders T3 and T4. This way a calibration curve is recorded for one half hour each day.

^{222}Rn is measured in air sampled via dedicated inlet lines at two heights of the tower, 20 and 200 m, by two independent dual flow loop, two-filter radon instruments,

designed and constructed at the Australian Nuclear Science and Technology Organisation (ANSTO) (Whittlestone and Zahorowski, 1998). The inlet flow rate is 80 l/min; each detector has a delay volume of 1500 l. From each height there is one data point every half hour, with the exception of few hours per month when the calibration is performed. The lower limit of detection, defined as the radon concentration corresponding to a relative counting error of 30 % for a one hour count, is equal to or less than 30 mBq/m^3. Calibrations of the radon detectors are performed monthly by injecting known amounts of radon into the inlet air stream from a calibrated radon source (Model 2000A, Pylon Electronics Inc., Canada). Calibration accuracy of the source is ±4 % at a 1-σ confidence level. For concentrations higher than 700 mBq/m^3 the overall uncertainly is predominantly attributed to the accuracy of the source.

2.3 Software

The RGA data are transferred at a frequency of 50 Hz to a PC equipped with PeakSimple™ chromatography software (SRI Instruments). PeakSimple™ performs the integration of the chromatographic peaks of interest according to a user-defined method, and creates reports containing the area, height and retention time of the peaks.

A custom-made Delphi software controls the overall measurement sequence and receives the data from the PeakSimple reports and from the other instruments. The Delphi software calculates the calibration parameters and the real-time mole fractions and writes data at different processing levels (raw and calibrated) into an Access database. Additional diagnostic parameters from various sensors (flows, pressures, temperatures) are registered for posterior data processing and quality check.

2.4 Data processing and quality control

A first quality check and flagging is performed on the raw data. Diagnostic parameters recorded in parallel with the signals from analyzer (flows, temperatures), and other information registered by operators (e.g. maintenance), are used to recognize the time intervals when the system did not perform well. The corresponding raw data are flagged as "bad" and will not be used further.

Next step is to compute the ratio between each measurement (peak area or height) and a "reference" measurement. We use as reference the interpolated value of the filtered (3-σ outliers removed) WT measurements. The ratios computed in this way are used for further calculation of mole fractions. The main purpose of this method is to correct for short and medium term variations of instrument sensitivity, due to for example variations of atmospheric pressure or room temperature. For both H$_2$ and CO, peak height has proven so far to give better results in terms of precision, especially during periods when the measurement was less stable.

The regular calibration consists in measuring the four calibration gases in a row. Calibration parameters are computed as a two degree least squares fit for each calibration. The calibration results are quality checked, and the ones considered bad are not used further. Next, a set of "virtual" calibration parameters are calculated for each point of the measurement time series, as a time-weighted moving average of all the good calibrations comprised into a time interval of 50 days around. These virtual calibration parameters are used for the calibration of the previously calculated ratios, in order to obtain the final mole fraction results.

3 Data coverage and quality

3.1 Coverage

The RGA measurements have been running without major interruptions since the end of September 2007. The number of existing data is about 94 % from the total possible number of data points, and about 91 % of the data obtained were considered good after the final quality check.

A leak affected intermittently the measurement from the 200 m sampling line for extended periods of time; the corresponding data have been identified and flagged as bad. Throughout this paper we therefore show data from the 200 m height for limited time intervals, but, in order to prevent biases due to different data coverage, we do not include data from this sampling height when describing general (average) features like seasonal cycles or diurnal cycles.

3.2 Precision

The long term repeatability of the Target measurement is a good estimator of the average analytical precision. The average precision of the RGA measurement at Cabauw, expressed as one standard deviation of all the Target results (over the whole measurement series), is about 3.5 ppb for both H$_2$ and CO. If we look at shorter time periods of days to weeks, the standard deviation of the Target results is typically 1.5 ppb for CO and 1.5 to 3 ppb for H$_2$. These latter values are the ones we will use throughout the rest of this paper when looking at short term signals.

3.3 Accuracy

High pressure cylinders are used in the atmospheric measurement community for inter-comparisons between different laboratories and field stations. We performed several intercomparison exercises with the MPI-BGC laboratory, using sets of three or four "travelling" cylinders within the projects CarboEurope IP (www.cucumbers.uea.ac.uk) and Eurohydros. The cylinders' mole fractions were in the approximate range of 450–650 ppb for H$_2$ and 100–400 ppb for CO.

For H$_2$, the average difference between the results at Cabauw and the MPI-BGC values was −0.9 ± 2.3 ppb, from

a total of 13 cylinders measured during 2008–2009. The average difference is not statistically significant, and the standard deviation is close to our typical precision. For CO, on the other hand, we found a statistically significant difference of 6.5 ± 2.7 ppb between Cabauw and MPI-BGC results. We could not detect so far a dependence of the differences between our results and MPI-BGC on the mole fractions for either H_2 or CO. Also, no time evolution of these differences was found, which is particularly important, as the intercomparison exercises took place before and after replacing one of the calibration gases in August 2009.

The intercomparison results demonstrated the accuracy of our H_2 calibration scale, but also helped to detect a systematic error between our results and the MPI-BGC ones, which is probably due to a shift in our CO calibration scale. Further investigation is necessary in order to document and eventually correct this problem, and intercomparison activities will be continued as an on-going verification.

4 Results and discussion

4.1 Data overview

Figure 3 shows the time series of H_2 and CO measured in air sampled at 20, 60 and 120 m above ground at Cabauw tall tower, since the start of measurements in September 2007 until October 2010. The measurement from the highest sampling height was not included here for the reasons explained in Sect. 3.1.

Both species show relatively high variability, due to the proximity of various sources and sinks. For H_2, the amplitude of the short term variations is typically on the order of 100 ppb during summer and 200 ppb during winter, but larger signals (500–600 ppb amplitude) can also be observed during winter. The variability of CO is strongly seasonal, primarily reflecting the large seasonality of the main CO sink – the reaction with the OH radicals, but also the seasonality of atmospheric mixing. The typical amplitude of the CO signals ranges from 100–200 ppb during summer to 300–500 ppb, with occasionally larger pollution events during winter.

4.2 Seasonal cycles of H_2 and CO

Seasonal cycles in both the "baseline" and the variability of H_2 and CO mole fractions are evident in Fig. 3. In order to describe the seasonal variations quantitatively, the 3-harmonics function shown below was fitted separately to the data from each sampling height by a linear least squares method.

$$f(x) = a_0 + \sum_{n=1}^{3}\left(b_n \sin\left(\frac{2\pi}{365}nx\right) + c_n \cos\left(\frac{2\pi}{365}nx\right)\right) \quad (1)$$

Because of the shortness of this data series, combined with large short term variability, it is not technically feasible to estimate an inter-annual trend. For that reason a linear component was not included in the function above.

The seasonal curves for H_2 and CO are shown in Fig. 4 in different colours for three sampling levels (20, 60 and 120 m); the data from the 200 m sampling height were not included for the reason explained in Sect. 3.1. For visual reference, we also show the time series from the 120 m sampling level. The dashed black lines show the seasonal variation of the "baselines"; these were computed from the 120 m level data by fitting the same seasonal function to the 5th percentile of the weekly afternoon data for H_2, and to the 3rd percentile of the monthly afternoon data for CO.

The general appearance of the seasonal curves of H_2 and CO is quite similar during winter and spring months, and becomes very different during summer. The mole fractions of both H_2 and CO increase sharply starting from October, until they reach the absolute maximum in January. They sharply decrease to an inflexion point in March, and after that is a steady period in April–May. Starting from May the two species have different behaviour. CO decreases sharply until it reaches the absolute minimum in July. H_2 has a slower decrease, and the minimum is reached three months later in October, while CO values are increasing again after the seasonal minimum. Nevertheless, the CO mole fractions seem to reflect somewhat the H_2 minimum in October, having an inflexion point around that time.

Similar to our results, Steinbacher et al. (2007) found a H_2 seasonal cycle with a maximum in winter, using data from another polluted continental site (Dübendorf, Switzerland). On the other hand, the H_2 seasonal cycles in background air masses at similar latitudes were shown to have the maximum later, in spring (e.g. Barnes et al., 2003; Bond et al., 2011; Ehhalt and Rohrer, 2009; Grant et al., 2010b; Novelli et al., 1999; Simmonds et al., 2000). If we look at the "baseline" curve in Fig. 4, we find the maximum in April, similar to the results from background stations.

There are three main factors contributing to the resulting H_2 seasonal cycle: the uptake by soil, the source from OH oxidation of hydrocarbons, and atmospheric circulation and vertical mixing; besides these, anthropogenic emissions are also weakly seasonal. During summer, the soil uptake dominates the net flux at this latitude (even if the local flux is small, see below), resulting in the autumn minimum observed at all stations. The spring maximum at background stations is due to accumulation over winter, when the soil sink is weak. At continental polluted sites like Cabauw and Dübendorf, in the presence of large emissions, the decrease in atmospheric mixing leads to large excursions in the mole fractions during winter, which in turn result in a shift of the maximum of the seasonal cycle towards this period; the effect is visible in the CO seasonal cycles as well. This explains the difference in the timing of maximum between continental and background stations, and between the average and "baseline" seasonal cycles at Cabauw and Dübendorf.
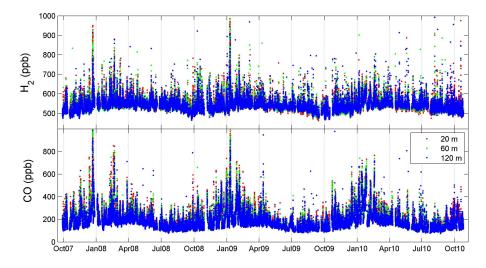
Fig. 3. Time series of H_2 and CO from three sampling heights. Different sampling heights are shown in different colours.
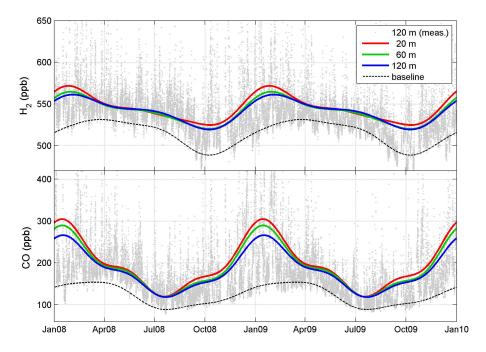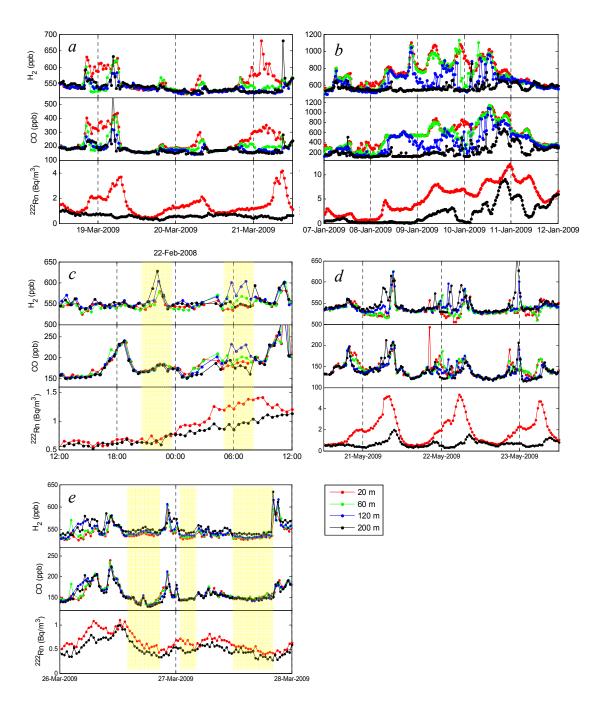

Fig. 4. Seasonal cycles of H_2 and CO at three sampling heights (colour lines) and the baseline at 120 m (black dashed line). Grey dots are the measurement series from 120 m sampling level.

The peak to peak amplitude of the H_2 seasonal cycle is slightly decreasing from about 47 ppb at the 20 m sampling height, to about 42 ppb at the 120 m sampling height. The CO seasonal cycle has the amplitude of about 186 ppb at 20 m sampling height, decreasing to about 148 ppb at 120 m sampling height. Larger seasonal amplitudes at the lower sampling heights are due to the proximity of sources and sinks that largely modulate the seasonal variations. The peak to peak amplitudes of the "baseline" curves are about 43 ppb for H_2 and 65 ppb for CO, similar to the results of Grant et al. (2010b) for background air masses, obtained from the

long term record at Mace Head, Ireland. We note however that the computed peak to peak amplitudes depend on the chosen data processing method; this should be taken into account when comparing these results with other studies.

4.3 Short term signals and vertical gradients

Characteristic short term signals and vertical gradients of various trace gases measured from tall towers have been described in the literature (e.g. Bakwin and Tans, 1995; Hurst et al., 1997). However not much information exists regarding

Fig. 5. Examples of H$_2$ and CO signals. **(a)** Evening and morning peaks during rush hours, and night time accumulation. **(b)** Large scale pollution event. **(c)** Pollution events detected at the highest sampling altitude (highlighted). **(d)** H$_2$ data from 20 and 60 m show night time depletion due to uptake by soil, while ^{222}Rn, continuously emitted by soil, is accumulating in the stable boundary layer. **(e)** Reversed H$_2$ gradient (highlighted).

the H$_2$ vertical gradients in the boundary layer. Several aircraft and balloon measurements have been reported (Cofer et al., 1986; Ehhalt et al., 1977; Fabian et al., 1979; Price et al., 2007; Schmidt, 1978; Seiler et al., 1978) but these are usually at higher altitudes, where the signals due to ground sources and sinks are smoothed out.

On short time scales, the variability of atmospheric concentrations is controlled by atmospheric circulation and vertical mixing, and by variations in source and sink fluxes in the influence area. The observed H$_2$ variations share some features with the other gas species, as they are affected by the same atmospheric transport and vertical mixing. Also,
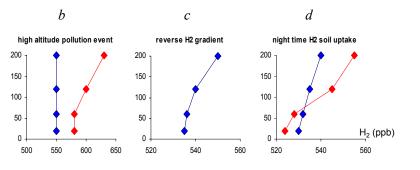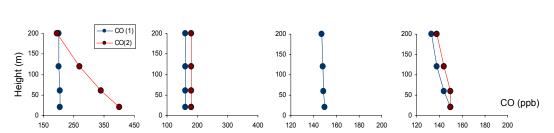
Fig. 6. Vertical profiles of H_2 (top) and CO (bottom) for various atmospheric situations. Except for plots **(c)**, vertical profiles before (blue) and during the event (red) are shown (see text for explanations). Note that the x-axis ranges are not the same for all plots, but the proportion between H_2 and CO ranges is maintained. **(a)** Local pollution event (night of 18–19 March 2009, see also Fig. 5a). **(b)** Pollution event at the highest sampling altitude (22 February 2008, see also Fig. 5c). **(c)** H_2 reverse gradient (27 March 2009, see also Fig. 5e). **(d)** Night time soil uptake of H_2 (21 May 2009, see also Fig. 5d).

the main H_2 sources in this region are anthropogenic, being common with other gas species, especially with CO.

However, unlike other trace species (e.g. CO, CH_4) that have sources near ground and sinks higher in the atmosphere, H_2 has both the main source (anthropogenic emissions) and the main sink (uptake by soil) in the lowest part of the troposphere. Species like CO and CH_4 show usually vertical gradients with higher mole fractions and higher variability near ground. In contrast, the vertical gradient of H_2 depends on the actual balance of sources and sinks near ground, and on the input from the higher atmosphere.

This section discusses different types of short term variations in H_2 mole fractions observed at Cabauw, and the corresponding vertical gradients. Figure 5 shows several selections of H_2, CO and ^{222}Rn data from different sampling heights, featuring typical short term signals. Figure 6 shows examples of vertical gradients corresponding to some common situations.

4.3.1 Local pollution signals

The most frequently observed variations in H_2 mole fractions are due to emissions from local or regional surface sources. These are seen as increases in mole fractions at the lowest sampling heights, and are largest during stable atmospheric conditions. Depending on the intensity of vertical mixing, the signal is sometimes transported, delayed and attenuated, to the higher sampling levels. In most cases a good correlation between H_2 and CO mole fractions shows that the excess

H_2 is of anthropogenic origin. (The correlation between H_2 and CO will be discussed in more detail in Sects. 4.6 and 4.7). Such pollution events last typically for a few hours but some situations have been observed when the accumulation of emissions lasted for several days.

An increase in mole fractions near ground can be driven by an increase in emissions, a decrease in atmospheric mixing, or a combination of the two. For example, we observe at Cabauw increases in H_2 and CO mole fractions during morning and evening traffic rush hours due to increase in emissions, as can be seen in Fig. 5a, for the evening of 20 March 2009 and the morning of 21 March 2009. On the other hand, during stable nights, the mole fractions increase near ground due to a decrease in vertical mixing, although the emissions typically decrease during night. Night time accumulations can be observed in Fig. 5a, during the nights of 18–19 March and 20–21 March 2009. Figure 5b shows a situation when an accumulation of trace gases lasted for several days, during an atmospheric blocking in the region.

4.3.2 Pollution events detected at the highest sampling altitude

A type of signal that is unusual for the other gas species is occasionally observed for H_2, that is, a sudden large increase in H_2 mole fraction at highest sampling levels (Fig. 5c). This increase is sometimes (but not always), transmitted towards the lower sampling levels. The H_2 signal can be mirrored by a correlated CO signal, but often during such events CO

mole fraction shows none or a smaller increase, and no similar large signals are observed in any of the other trace species measured. The origin of these signals is unclear, but we suspect emissions from a tall industrial chimney in the region or low flying airplanes. The sharpness and amplitude of these signals show that the source cannot be very far.

4.3.3 Local soil sink signature

Uptake by soil represents one of the largest H_2 fluxes over the continental areas. It is therefore expectable that soil uptake would influence the mole fractions and the vertical gradients measured at a continental site. Previous studies (e.g. Hammer and Levin, 2009; Yver et al., 2009) reported decreases of H_2 mixing ratios near ground, which were attributed to soil uptake during night time stable atmospheric conditions. In such cases, the CO mole fractions measured in parallel show no significant decrease, and the ^{222}Rn increases due to accumulation from the soil efflux.

At Cabauw we observe similar soil uptake signals, i.e. night time H_2 depletion at lowest sampling heights, but more seldom than at other continental stations. This is because the local and regional anthropogenic emissions are large and often dominate the net flux, and because the atmospheric mixing conditions in the Netherlands tends to be less stable than at more continental locations. However, even when an absolute decrease in H_2 mole fraction is not very evident, we often observe a relative depletion in H_2 at low sampling levels compared to the high sampling levels, as can be seen in Fig. 5d.

4.3.4 Reversed H_2 vertical gradients (H_2 increase with sampling height)

Besides the night time local soil uptake signals, we observe another interesting feature in the H_2 vertical profiles, as exemplified in Fig. 5e. Under certain atmospheric conditions, usually when the air column is relatively well mixed and not very polluted, H_2 has a small and relatively constant vertical gradient with higher mole fractions at higher sampling heights; the difference between the highest and the lowest sampling heights is usually of 5–10 ppb. During such intervals, the ^{222}Rn has a small opposite gradient, with higher values at 20 m. The other species measured either show no gradient, or a small gradient with higher values near ground, similarly to ^{222}Rn.

We initially suspected a contamination with room air, as the room air has usually a high H_2 concentration due to a continuously operating H_2 generator. However the H_2 generator was stopped during two periods in 2009, between 17 March and 22 April, and between 17 June and 2 September. During these intervals, when a contamination could not be the cause, the systematic difference between the 200 m and the other sampling levels persisted, as shown in Fig. 5e.

There are no similar measurements in the lowest few hundred meters of the troposphere to compare our results with. Some of the few reported aircraft observations made at middle to high northern latitudes found an increase of H_2 with altitude, with a maximal vertical gradient in summer-fall (Cofer et al., 1986; Price et al., 2007; Schmidt, 1978). Modeling studies (Hauglustaine and Ehhalt, 2002; Pieterse et al., 2011) predicted large vertical gradients at these latitudes as well, with strong H_2 depletion towards surface during summer. These however do not cover the lowest part of the planetary boundary layer with high resolution. Our dataset does not show any clear evidence of seasonality in the H_2 vertical profiles.

We interpret these systematic vertical gradients as possibly due to a large scale influence of soil uptake at this latitude.
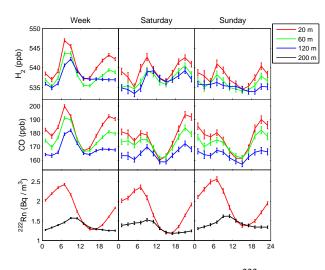
4.3.5 Vertical gradients summary

Figure 6 summarizes the vertical profiles of H_2 and CO, as observed at Cabauw for the typical situations described above. Plots 6a show the correlated increase in H_2 (top) and CO (bottom) before and during a local pollution situation with near-ground accumulation for both species (night of 18–19 March 2009, see also Fig. 5a). Plots 6b show the CO and H_2 vertical profiles before and during a pollution event at the highest sampling level for H_2, when CO did not follow a similar evolution (see also Fig. 5c). Plots 6c show the CO and H_2 gradient during a situation of "reversed H_2 gradient" (27 March 2009, see also Fig. 5e). Finally, plots 6d show the evolution of CO and H_2 vertical profiles during the night of 21 May 2009, when CO was slowly accumulating, while H_2 was depleted near ground due to local soil uptake, resulting in a relatively large H_2 vertical gradient (see also Fig. 5d).

In summary, the observations at Cabauw show that the H_2 mole fractions and vertical gradients in the continental boundary layer are highly variable over short time intervals, due to overlapping influences of soil sink, emissions from anthropogenic sources and atmospheric transport and vertical mixing. Thus high frequency atmospheric observations made at different sampling heights are necessary for obtaining a representative picture.

4.4 Diurnal cycles

The average diurnal cycles of H_2, CO and ^{222}Rn, calculated separately for weekdays, Saturdays and Sundays are shown in Fig. 7. Diurnal cycles of atmospheric constituents are due to both the periodicity of fluxes, and the periodicity of the atmospheric circulation, especially of the vertical mixing. The ^{222}Rn plots in Fig. 7 help to distinguish between these two influences on the H_2 and CO diurnal cycles, as we expect that the average ^{222}Rn concentration depends mainly on the atmospheric vertical mixing.

Fig. 7. Average diurnal cycles of H_2, CO and ^{222}Rn, for weekdays, Saturdays and Sundays. Each data point is the trimmed average (discarding the 10 % lowest and highest values) of a 2-hourly bin. The data between 03:00 and 04:00 were excluded, because the daily calibration took place mostly during this interval, thus the results were possibly biased. For H_2 and CO, the data from the 200 m height are not shown for the reason explained in Sect. 3. The error bars are standard errors of the means corresponding to 67 % confidence intervals.

On the diurnal scale, the variability of CO and H_2 is dominated by large mole fraction increases during the morning and evening peaks of human activities, mainly traffic. The peaks are largest at 20 m, and appear attenuated and slightly delayed at the higher sampling levels. The morning peak is sharper, as it starts during the time when the vertical mixing is poor, and it terminates abruptly at the morning onset of the vertical mixing. The afternoon peak starts while the vertical mixing is still relatively strong, thus the mole fraction increases are slower.

There is an obvious difference between the weekday and weekend diurnal cycles of H_2 and CO, as similarly observed at other polluted sites by e.g. Steinbacher et al. (2007) and Yver et al. (2009). Although attenuated, the difference between weekday and weekend appears at higher sampling heights as well, suggesting that this is not only local, but a larger scale effect. As expected, no significant difference between weekday and weekend is observed in the ^{222}Rn diurnal cycles.

The morning peak is largest during weekdays, and it attenuates on Saturday and further on Sunday. The attenuation appears to be larger for CO, which on Sunday morning has an inflexion point, but no significant mole fraction increase at the lowest sampling height.

The H_2 evening peak decreases from weekdays to Saturday and Sunday, and it is slightly delayed during the weekend. In contrast, the CO evening peak has an increasing tendency during weekend, when compared to the afternoon

dip level. A similar feature can be observed in Yver et al. (2009), in their Fig. 6, with a CO evening peak increasing during weekend, while H_2 evening peak showed no increase. We propose the following explanation. During weekend, the evening and night traffic increases, but (unlike during working days) there are no afternoon commuter traffic jams, which leads to a more fluent driving regime. H_2/CO ratios are higher during jammed rush hours, when the frequent acceleration leads to an increase in H_2 emissions due to an altered combustion chemistry in fuel-rich and oxygen-deficient conditions, and to a poorer catalytic removal of H_2 (Vollmer et al., 2007, 2010). Traffic jams occur regularly during working days on the Dutch main roads, especially in the Utrecht area which is not far from our site. The H_2/CO ratios during weekdays are therefore affected by larger H_2 emissions relative to CO during rush hours, while the weekend ratios, with lower H_2 relative to CO, are more representative for fluent traffic conditions (see also Sect. 4.6). Note that the larger CO evening peak during weekend does not necessarily imply larger emissions; the weekend evening peak occurs later, when the atmospheric mixing is lower, thus the larger increase in mole fractions is probably due to weaker vertical dilution.

The afternoon dip in both H_2 and CO is mainly due to vertical mixing, although the decrease in emissions after the morning peak contributes as well. As also observed by Steinbacher et al. (2007), the CO afternoon minimum at 20 m sampling height is more pronounced than the night time minimum, whereas for H_2 the two minima have approximately the same level. The reason is that both CO minima are mainly due to dilution by cleaner air from the free troposphere, and this dilution is much stronger during day. The H_2 night time minimum has in addition a contribution from soil uptake, which further decreases the mole fraction to a level comparable to that of the afternoon minimum.

4.5 H_2 soil sink

^{222}Rn is a natural radioactive noble gas with a half-life time of 3.8 days, which is exhaled continuously from the ground. Its only non negligible sink mechanism is radioactive decay. This makes ^{222}Rn a good tracer for atmospheric transport and evaluation of the extent to which an air parcel has been in contact with the soil in the past few days.

The radon tracer method was first proposed by Levin (1984), and it has since been used to determine fluxes of various trace gases at local to continental scale (e.g. Biraud et al., 2000; Gaundry et al., 1990; Levin et al., 1999; Messager et al., 2008; Schmidt et al., 2001, 2003; Wilson et al., 1997). The concept is comprehensively described in e.g. Schmidt et al. (2001), and Hammer and Levin (2009) (also Levin, 1984, in German). In essence, the method uses the correlation, during stable atmospheric conditions, between variations in concentration of ^{222}Rn and of the trace gas of interest. Based on this correlation, and assuming that the flux

of ^{222}Rn is known and constant, it is possible to compute the net flux of the trace gas studied.

Several recent studies employed the radon tracer method to determine the night time H_2 soil uptake rates at different European locations: Heidelberg, Germany (Hammer and Levin, 2009), Gif-sur-Yvette, France (Yver et al., 2009), Helsinki and Pallas, Finland (Lallo et al., 2009a, b). The reasoning for using the radon tracer method to infer the soil uptake of H_2 is as follows. During the nights with stable atmospheric conditions, ^{222}Rn that is emitted by soil at a relatively constant rate will accumulate in the boundary layer. For H_2, the only significant sink during night is soil uptake. If the concurrent H_2 emission is smaller than the absolute value of the soil uptake flux, H_2 levels in the boundary layer will decrease. The net flux of H_2 can be computed from the observed ratio of the variations in H_2 and ^{222}Rn concentrations, using the equation:

$$F_{H_2} = F_{Rn} \frac{\Delta C_{H_2}}{\Delta C_{Rn}} \tag{2}$$

where F_{H_2} is the net flux of H_2 into the boundary layer; F_{Rn} is the net flux of ^{222}Rn; and ΔC_{H_2} and ΔC_{Rn} are the measured variations in concentration of H_2 and ^{222}Rn. F_{Rn} includes the ^{222}Rn emission from soil and the loss by radioactive decay, and it can be computed as follows:

$$F_{Rn} = F_{Rn\_soil} + F_{Rn\_decay} = F_{Rn\_soil} \left(1 - \frac{\lambda}{\Delta C_{Rn}} \int_{\Delta t} C_{Rn}(t) \, dt \right) \tag{3}$$

In the equation above, λ is the decay constant of ^{222}Rn, C_{Rn} is the instantaneous ^{222}Rn concentration, and Δt is the time interval considered for calculation.

The method can only be applied when a stable nocturnal boundary layer is formed, as in that case the exchange between the boundary layer and the layer above it can be considered negligible.

In order to infer the H_2 soil uptake in the influence area of Cabauw tall tower station using the radon tracer method, we proceeded as follows. First, we selected all nights when simultaneous H_2 depletion and ^{222}Rn increase could be observed at the 20 m sampling height. From these, only the nights when the H_2 mole fraction at 20 m decreased below the H_2 mole fraction at the higher sampling heights were considered.

As discussed by e.g. Moxley and Cape (1997), it is important that the mole fraction at the start of the decline is typical for the background, and declines below this level at night, otherwise a decrease in emission could be erroneously interpreted as soil sink. We paid therefore special attention to exclude those situations when the H_2 was decreasing towards the background value after an evening pollution event, and the synoptic variations.

Based on these criteria, 84 nights were selected from the whole measurement series. For each of the selected nights,

the exact time interval was chosen after careful visual inspection. For these periods we computed the H_2:^{222}Rn ratio, as a slope of a linear least square fit that minimizes the residuals on both x and y axes, taking into account the assigned uncertainties for both x (H_2) and y (^{222}Rn) (York et al., 2004). For H_2 data we assigned a constant error of 1.5 ppb, based on the repeatability of the Target measurement during the period of interest. For ^{222}Rn data we assigned a constant relative error of 4 %, based on the average standard deviation of the half-hourly counts. We assumed a constant ^{222}Rn soil flux of 0.29 ± 0.1 atom/(cm^{2}s) (16 ± 5 Bq/(m^{2}h)), which is the average for the Netherlands for the year 2006 as reported by Szegvary et al. (2007a). The correction for the radioactive decay of ^{222}Rn was made according to Eq. (3), and the H_2 flux was computed using Eq. (2).

For 18 of the selected nights a correction for concurrent anthropogenic emissions was applied, based on the parallel CO measurements. During these nights, CO was increasing, indicating that the emissions were significant. The CO flux was computed using the radon tracer method, and a correction for the H_2 soil flux was computed by scaling the CO flux with a factor of 0.5 mol:mol. For the CO data we assigned a constant error of 1.5 ppb.

The estimated errors represent the result of combined ^{222}Rn flux error with the individual slope errors and with the error resulted from the correction for concurrent emissions.

A final check was performed, eliminating the nights which did not fulfill the following conditions: (1) the Pearson correlation coefficient r of the H_2 and ^{222}Rn data (in absolute value) at least 0.5; (2) the relative error of the H_2:^{222}Rn slope smaller than 25 % (3) the H_2 range minimum 2 ppb; (4) the ^{222}Rn range minimum 0.1 Bq/m^3; (5) at least 4 half-hourly data points for both H_2 and ^{222}Rn; (6) the combined H_2 soil flux error smaller than 2×10^{-5} g/(m^{2}h). A number of 66 nights remained after this final selection.

The H_2 soil flux results are presented in Fig. 8. There were no deposition events that passed the selection criteria during winter, and there are only a few data points in 2008. This is due to the high atmospheric instability in the Netherlands, and to the high anthropogenic emissions which most of the time dominate the net flux of H_2.

Some structure can be observed, for example an increasing tendency in May–June 2009, and a decrease in flux in autumn 2009. Although this is consistent with a seasonal variation of the soil uptake, which has been observed before at other sampling sites (e.g. Hammer and Levin, 2009; Lallo et al., 2008; Yver et al., 2009), it is obvious that we cannot draw a strong conclusion based on this dataset. This variation may as well be a short term feature, related to the weather conditions during the respective months.

The average H_2 flux is $(-1.89 \pm 0.26) \times 10^{-5}$ g/(m^2 h) (the $\pm$ values through the paper are the 95 % confidence intervals for the mean); as the distribution is asymmetrical, the median is probably more informative (-1.59×10^{-5} g/(m^2 h)). The corresponding deposition
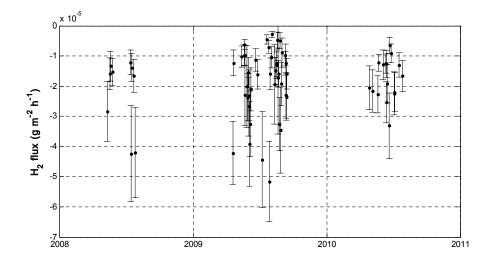
Fig. 8. H_2 soil deposition flux calculated with the ^{222}Rn tracer method for selected deposition events.

velocity average is $(11.4 \pm 1.54) \times 10^{-3}$ cm/s (the median is 9.8×10^{-3} cm/s). Note that these results cannot be viewed as annual averages, since there are no data during the cold months when the soil uptake is likely to be smaller.

The mean H_2 deposition flux (and the resulting deposition velocity) we obtained is significantly smaller than most other results from European sites recently reported in literature. Yver et al. (2009) found an average flux of -4.26×10^{-5} g/(m^2 h) at Gif-sur-Yvette, a rural site near Paris. Hammer and Levin (2009) and Schmidt et al. (2009) reported flux values of -4.6 g/(m^2 h) and an annual mean deposition velocity of about 30×10^{-3} cm/s at Heidelberg, Germany. Lallo et al. (2008, 2009a, b) studied the H_2 soil uptake at several sites in Finland and found the H_2 deposition velocity ranging mainly between 10 and 60×10^{-3} cm/s with a significant seasonality. Steinbacher et al. (2007) found a range of 5–10×10^{-3} cm/s near Zurich in Switzerland, and Grant et al. (2010a) computed from only winter time data an average of 22×10^{-3} cm/s from Bristol, UK.

There are two main factors that could have potentially contributed to the small H_2 fluxes we obtained. First, it is likely that the soil uptake in the Cabauw area is indeed smaller than in other areas in Europe. The soil at Cabauw is peat, and the water content is relatively high. Previous studies found a decrease of the H_2 uptake with the increase in soil moisture above 20–30 % whc (Conrad and Seiler, 1981; Gödde et al., 2000; Smith-Downey et al., 2006).

Second, the ^{222}Rn flux from Szegvary et al. (2007a) for the Netherlands of 0.29 atom/(cm^{2}s) is very small compared to other countries in the area. Also, this flux was computed for the year 2006 and does not account for interannual variability. Moreover, the short term variability of ^{222}Rn emissions can be large (see Szegvary et al., 2007b, Fig. 3, where the variation over few weeks during summer was approximately between 20 and 100 Bq/(m^2 h)). The ^{222}Rn flux de-

pends on the soil moisture (Szegvary et al., 2007b, and references therein), being higher under dry conditions. As we chose only stable nights, which are drier than the average, the real ^{222}Rn flux during these nights is probably higher than the average. For these reasons, we suspect that the average value of 0.29 atom/(cm^2 s) is an underestimation of the real ^{222}Rn flux during the intervals selected for our calculation, which leads to an underestimation of the H_2 soil uptake fluxes.

This is supported by a simple ^{222}Rn flux estimation we made based on the in-situ ^{222}Rn measurements. After a well mixed afternoon situation, the vertical mixing decreases during stable nights, and ^{222}Rn accumulates in the shallow boundary layer. In such cases, we observe an increase in ^{222}Rn concentrations at 20 m, while there is no increase (or even a slight decrease) at 200 m. In order to compute the ^{222}Rn flux, we assume that no ^{222}Rn is transported above the 20 m level, and that the layer between 0 and 20 m is uniform (both assumptions will lead to an underestimation of ^{222}Rn flux). If the accumulation time is 8 h, and ^{222}Rn reaches at the end of this time a value of 8 Bq/m^3 (which is typical during stable nights, but not the maximum), then the ^{222}Rn flux required is 0.36 atom/(cm^2 s) (or 20 Bq/(m^2 h)). This is a lower limit value, because in fact some of the emitted ^{222}Rn is certainly transported above the 20 m height, and because the concentration near ground is higher than at 20 m. Even with these limitations, the ^{222}Rn flux calculated for individual nights is up to 0.6 atom/(cm^2 s). Although this is a simplistic approach, it shows that the ^{222}Rn fluxes in the Cabauw area can be in certain conditions significantly higher than the average value of 0.29 atom/(cm^2 s) given by Szegvary et al. (2007a).

In summary, because the value used for the ^{222}Rn flux likely leads to an underestimation of the H_2 soil flux, we think that our results could represent a lower limit of the real H_2 soil uptake flux in the region. It would be useful to
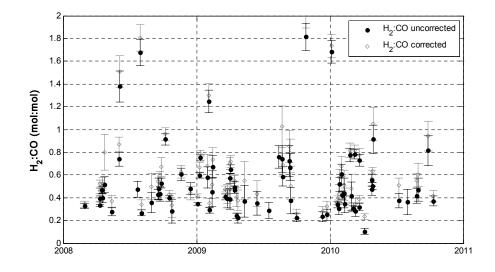
Fig. 9. Molar H_2/CO ratios from morning rush hour data. For comparison, the data before and after the H_2 soil uptake correction are shown.

compare direct soil flux measurements from chambers with results derived from the tall tower data.

4.6 H_2/CO ratios from traffic emissions

In order to derive the H_2/CO ratios specific to traffic emissions, we followed an approach similar to Hammer et al. (2009) and Yver et al. (2009), adapted to the particularities of our site and data.

Because the traffic peaks depend on local time (while our measurement system uses GMT), we considered the time intervals 04:00 to 06:30 GMT during summer (equivalent to 06:00–08:30 local time) and 05:00 to 07:30 GMT during winter (06:00–08:30 local time). We selected the mornings with monotonous increase in H_2, CO and ^{222}Rn at 20 m sampling height during this interval. From these, we only chose those mornings when the presence of significant vertical gradients in ^{222}Rn (between 20 m and 200 m) showed that the vertical mixing is weak. This second selection is necessary in order to exclude large scale synoptic events like frontal system passages. For each of the selected mornings we computed the H_2/CO ratio by a least squares fit, as described in Sect. 4.5. The results were then filtered using the following criteria: (1) the correlation coefficient r had to be larger than 0.8; (2) the absolute slope error had to be smaller than 0.15 mol:mol, and the relative slope error smaller than 40 %; (3) the increase in CO and H_2 had to be larger than 10 ppb respectively 5 ppb.

The H_2/CO ratios we obtained for the 85 mornings that passed these criteria are shown in Fig. 9. The mean H_2/CO ratio is 0.54 ± 0.07 mol:mol, with a standard deviation of 0.32 mol:mol and a median of 0.45 mol:mol.

We computed for comparison the H_2/CO ratio for the morning peak of the average diurnal cycle (see Fig. 7). If we only consider the working days data and the 20 m sam-

pling height, we obtain a H_2/CO ratio of 0.46 over the time interval 04:00–06:30, which is comparable with the discrete results presented above.

Our results for the traffic H_2/CO ratio are higher and more variable than some of the previously reported results of similar calculations in Europe. For example, the results of Steinbacher et al. (2007) and Yver et al. (2009) from Dübendorf, Switzerland, and Gif-sur-Yvette, France, are very similar to each other (0.33 mol:mol), but different from our results; Hammer et al. (2009) observed H_2/CO ratios of 0.40 mol:mol at Heidelberg. Although we found some values around 0.3–04 mol:mol, this seems to be the lower limit of the range, and about 40 % of our results are higher than 0.5 mol:mol. Grant et al. (2010a), on the other hand, reported H_2/CO ratios as high as 0.57 for the morning traffic peaks (and 0.53 for all data) using winter time measurements at an urban site in UK.

Hammer et al. (2009) showed that directly measured H_2/CO ratios are not fully representative for the traffic emissions, unless corrected for the concurrent soil fluxes of CO and H_2. At our site, however, the 20 m sampling level can be, in the early morning when the vertical mixing is minimal, above the local mixed layer. Even in these conditions we observe traffic signals, horizontally transported from surrounding areas with high traffic, where the atmospheric turbulence is enhanced and the influence of the soil uptake is insignificant. It is thus possible to sample air masses that were strongly influenced by traffic emissions but little affected by soil uptake. We consider therefore the soil correction at Cabauw less meaningful than at the sites where it was previously applied by Hammer et al. (2009) and Yver et al. (2009).

Keeping the above in mind, we applied a correction for the soil sink to our results, as an exercise and for comparison with previous studies. We used a method similar to the
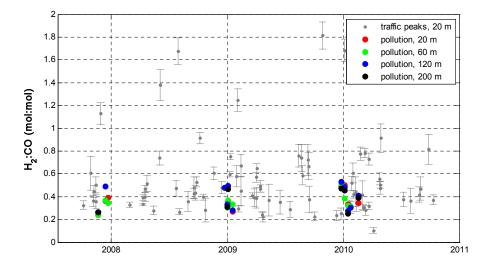
Fig. 10. H_2/CO ratios of large scale pollution events, for the four sampling heights. Overlapped are the ratios of the morning traffic peaks, for comparison. The results are not corrected for the concurrent soil uptake.

one of Hammer et al. (2009) and Yver et al. (2009). We considered the soil uptake of CO negligible, and for the H_2 soil flux we used the values estimated in Sect. 4.5, of $(-1.89 \pm 0.26) \times 10^{-5}$ g/(m^2 h) during the warm season and an arbitrary value of $(-1 \pm 0.26) \times 10^{-5}$ g/(m^2 h) during the cold season. The CO traffic flux (approximately equal to the total flux) was computed applying the radon tracer method to the individual selected morning intervals. The corrected H_2/CO ratios (grey markers in Fig. 9) yield an average of 0.63 ± 0.27 mol:mol, with a median of 0.54, thus the soil correction increased the H_2/CO ratios by about 18 %. We consider that the corrected values show the upper boundary of the real H_2/CO ratios specific to the local traffic, while the uncorrected results show the lower boundary.

Previous recent results reported in Europe, computed in a similar manner and corrected for the H_2 soil sink, are: 0.46 ± 0.7 (Hammer et al., 2009) and 0.47 ± 0.08 (Yver et al., 2009). Vollmer et al. (2007) measured emission ratios in a highway tunnel near Zürich, and obtained a mean H_2/CO ratio of 0.48 ± 0.12; in this case the correction for the H_2 soil sink was not necessary. Our results are (as expected from the uncorrected results) larger than these other estimates.

Vollmer et al. (2010) studied emissions from a passenger car engine, and showed that the absolute quantities of H_2 and CO emitted, and the H_2/CO ratio depend on the operational regime. They found that exhaust H_2 concentrations (after catalyst) decrease below the atmospheric H_2 concentrations in fuel lean functioning conditions; if this is the general rule, then fluent traffic should not have a large impact on the atmospheric H_2 mole fractions (while still affecting atmospheric CO). It follows that the large H_2 mole fraction increases observed during morning rush hours are mainly due to engines operating in fuel-rich combustion conditions, which, according to the same study, emit much larger quantities of H_2 and

CO, and, depending on the air-fuel ratio, potentially higher H_2/CO ratios of up to 1.5. As mentioned above, traffic congestions are common in the Netherlands especially during rush hours. This supports our conclusion that the driving regime, which is slow and irregular during the rush hours, is the main explanation for the high H_2/CO ratios.

4.7 H_2/CO ratios from pollution events

Besides H_2/CO ratios from traffic emissions, we investigated the ratios in large scale pollution events. We selected for this a number of large pollution events that start from mole fractions close to the baseline, that cover at least 24 h and for which the preliminary visual inspection indicates a good correlation between H_2 and CO. We computed, separately for the four sampling heights, the H_2/CO ratios as slopes of a least squares fit, similarly to the ratios for the traffic peaks described before (fitting method described in Sect. 4.5).

After computing the H_2/CO slopes, we removed the ones for which the H_2/CO correlation was lower than 0.7 or the error of the computed slopes was larger than 0.1. The remaining 13 events are all during winter (Fig. 10). This reflects the fact that H_2 and CO are, during summer, well correlated on short term (like during evening and morning traffic pollution peaks) but the correlation decreases for intervals longer than several hours, due to soil uptake of H_2 and stronger atmospheric mixing.

The resulting H_2/CO ratios tend to be larger at higher sampling heights (probably due to a stronger soil sink influence near ground), but this is not a strict rule, and the variation with sampling height is not monotonous. The mean H_2/CO ratios for the sampling heights of 20, 60, 120 and 200 m are: 0.36 ± 0.05, 0.37 ± 0.04, 0.40 ± 0.06, and 0.37 ± 0.07 mol:mol. It can be seen that on average, both

the H_2/CO ratio and the spread of the results increase with sampling height.

The H_2/CO ratios for the large scale pollution events are on average lower than the ratios for the traffic peaks; they are also less variable, somewhat surprisingly as they are from a combination of different sources and influence areas. The lower variability of H_2/CO ratios during large scale events is probably more representative for the integrated regional to continental emissions, and suggests that the large spread we found in the case of traffic emission ratios is a smaller scale feature related to the local traffic conditions.

The values we found for the lowest sampling height, of 0.36 ± 0.05 mol:mol, are close to other results from continental Europe; e.g. Hammer et al. (2009) obtained an average of 0.31 ± 0.05 mol:mol for synoptic events, and Steinbacher et al. (2007) computed an overall ratio of 0.33 mol:mol.

5 Summary and concluding remarks

Atmospheric H_2 has been measured at the tall tower Cabauw since September 2007. H_2 is measured in air alternately sampled from four heights of the tower, between 20 and 200 m, in parallel with other trace gas species: CO, CO_2, CH_4, N_2O and SF_6. ^{222}Rn measurements are performed in air sampled at 20 and 200 m. The long term precision of the RGA measurement, estimated from the repeatability of a Target cylinder measurement, is about 3.5 ppb for both H_2 and CO.

From three years of data, we were able to determine systematic features and variability patterns on various time scales. Seasonal cycles are present in both H_2 and CO time series, and their amplitudes vary with the sampling height. The short term variability is also changing with season; larger variability during winter is explained by seasonality of the atmospheric transport and, in the case of CO, also by seasonal variations in the atmospheric lifetime, controlled by the OH radical concentration.

Unlike most other trace gases, H_2 has in this area both the main source and the main sink near ground level. This causes specific features of the short term signals and of the vertical gradients. During short term pollution events, like the evening and morning peaks due to traffic emissions, H_2 vertical gradients and the variations in mole fraction are strongly correlated to the ones of CO. Outside these short intervals with intense emissions, H_2 variations in mole fractions are not always associated to similar variations in CO mole fractions. Unexpected large H_2 signals have been observed, typically at the higher sampling levels, for which CO showed much smaller or even no increases; the origin of these signals is unclear.

The H_2 soil sink plays an important role in determining the atmospheric H_2 mole fractions. The local soil sink is responsible for the H_2 depletion near ground during stable nights, associated with a reversed H_2 vertical gradient compared to CO. Vertical gradients of H_2 with slightly higher mole frac-

tions at highest sampling levels can be observed also during less stable atmospheric conditions, when the air masses receive influences from a wider area; these vertical gradients can probably also be explained by soil uptake, but on a much larger spatial scale than the nocturnal depletions.

We estimated the H_2 soil sink flux in the footprint of the 20 m sampling level, using the radon tracer method similarly to other recent studies in Europe. Due to the generally high atmospheric instability in the area, and to our strict data selection criteria, we could only perform this flux estimation for warm season nights, between April and September. The average of all individual results obtained is $(-1.89 \pm 0.26) \times 10^{-5}$ g/(m^2 h), significantly smaller than other recent results from Europe. There are two possible (partial) explanations for this difference. The soil characteristics in the Cabauw area, together with the high water content can probably explain a somewhat smaller than average soil uptake. Also, our result relies critically on the average value of ^{222}Rn flux for the Netherlands derived from Szegvary et al. (2007a), which is significantly smaller than values reported for other areas in Europe, and, being an annual average, might not represent well the real ^{222}Rn fluxes during the time of our estimation.

Diurnal cycles in atmospheric H_2 and CO are due to a combination of atmospheric vertical mixing and periodicity in emissions. Both H_2 and CO diurnal cycles show evening and morning peaks associated to road traffic emissions. Differences between weekdays, Saturdays and Sundays are clearly visible in the diurnal cycles of both species. However the evolution over the week time of H_2 and CO is not identical, which points to different proportions of H_2 and CO emitted in various traffic conditions.

The H_2/CO ratios for the morning traffic peaks are more variable and on average higher than previous results from Europe. The difference can probably be explained by a different driving regime, due to the frequent traffic jams in the influence area of Cabauw. In contrast, the H_2/CO ratios of the large scale pollution events are similar to results of previous studies (e.g. Hammer et al., 2009; Steinbacher et al., 2007); these ratios were observed to slightly increase with the sampling height, possibly due to a stronger influence of soil uptake at the lower sampling heights.

The highest sampling levels at Cabauw have a large average influence area, as estimated by Henne et al. (2010) and further discussed by Vermeulen et al. (2011). Vermeulen et al. (2011) show that the average influence area for the 200 m sampling level is roughly 500×700 km around, covering large part of West Europe, while the 20 m sampling level receives a relatively larger influence from local emissions. The representativeness of particular results is however dependent on the data selection and analysis method. For example, depending on how we process the data, we can extract from our data series seasonal cycles representative for the background air at the latitude of the Cabauw tall tower, or for continental polluted air. The results for the H_2 soil

uptake and for the H_2/CO ratios of the traffic emissions are based on short term (several hours) signals at the lowest sampling heights and thus are largely influenced by fluxes within few tens of kilometers. On the other hand, the H_2/CO ratios for the larger pollution events are representative for a wider area, which probably explains the closer similarity with results from other locations in Europe.

This data set represents the first in-situ, quasi-continuous, long term measurement of vertical profiles of H_2 in the lower continental boundary layer. It provides a wealth of information of sources, sinks and processes affecting atmospheric H_2. The mole fraction data coupled with inverse models will be used to derive regional fluxes of H_2. The location in Western Europe is suitable for monitoring from the start the effects of a large scale introduction of H_2 as an energy carrier; for this, the measurements have to be continued on long term.

Edited by: C. Gerbig

References

Aalto, T., Lallo, M., Hatakka, J., and Laurila, T.: Atmospheric hydrogen variations and traffic emissions at an urban site in Finland, Atmos. Chem. Phys., 9, 7387–7396, doi:10.5194/acp-9-7387-2009, 2009.

Bakwin, P. S. and Tans, P. P.: Measurements of carbon dioxide on a very tall tower, Tellus, 47B, 535–549, 1995.

Barnes, D. H., Wofsy, S. C., Fehlau, B. P., Gottlieb, E. W., Elkins, J. W., Dutton, G. S., and Novelli, P. C.: Hydrogen in the atmosphere: Observations above a forest canopy in a polluted environment, J. Geophys. Res.-Atmos., 108, 4197, doi:10.1029/2001JD001199, 2003.

Biraud, S., Ciais, P., Ramonet, M., Simmonds, P., Kazan, V., Monfray, P., O'Doherty, S., Spain, T. G., and Jennings, S. G.: European greenhouse gas emissions estimated from continuous atmospheric measurements and radon 222 at Mace Head, Ireland, J. Geophys. Res., 105, 1351–1366, 2000.

Bonasoni, P., Calzolari, F., Colombo, T., Corazza, E., Santaguida, R., and Tesi, G.: CO and H_2 continuous measurements at Mt.Cimone (Italy): Preliminary results, Atmos. Environ., 31, 959–967, doi:10.1016/S1352-2310(96)00259-2, 1997.

Bond, S. W., Alvarez, R., Vollmer, M. K., Steinbacher, M., Weilenmann, M., and Reimann, S.: Molecular hydrogen (H_2) emissions from gasoline and diesel vehicles, Sci. Total Environ., 408, 3596–3606, doi:10.1016/j.scitotenv.2010.04.055, 2010.

Bond, S. W., Vollmer, M. K., Steinbacher, M., Henne, S., and Reimann, S.: Atmospheric molecular hydrogen (H_2): Observations at the high altitude site Jungfraujoch, Switzerland, Tellus B, 64–76, doi:10.1111/j.1600-0889.2010.00509.x, 2011.

Bousquet, P., Yver, C., Pison, I., Li, Y. S., Fortems, A., Hauglustaine, D., Szopa, S., Rayner, P. J., Novelli, P., Langenfelds, R., Steele, P., Ramonet, M., Schmidt, M., Foster, P., Morfopoulos, C., and Ciais, P.: A three-dimensional synthesis inversion of the molecular hydrogen cycle: Sources and sinks budget and implications for the soil uptake, J. Geophys. Res., 116, D01302, doi:10.1029/2010JD014599, 2011.

Cofer III, W. R., Harriss, R. C., Levine, J. S., and Edahl Jr., R. A.: Vertical distributions of molecular hydrogen off the eastern and Gulf coasts of the United States, J. Geophys. Res., 91, 14561–14567, 1986.

Conrad, R.: Soil Microbial Processes and the Cycling of Atmospheric Trace Gases, Royal Society of London Philosophical Transactions Series A, 351, 219–230, 1995.

Conrad, R.: Soil microorganisms as controllers of atmospheric trace gases (H_2, CO, CH_4, OCS, N_2O, and NO), Microbiology and Molecular Biology Reviews, 60, 609–640, 1996.

Conrad, R. and Seiler, W.: Decomposition of atmospheric hydrogen by soil microorganisms and soil enzymes, Soil Biol. Biochem., 13, 43–49, 1981.

Conrad, R. and Seiler, W.: Influence of Temperature, Moisture, and Organic Carbon on the Flux of H_2 and CO Between Soil and Atmosphere: Field Studies in Subtropical Regions, J. Geophys. Res., 90, 5699–5709, 1985.

Constant, P., Poissant, L., and Villemur, R.: Annual hydrogen, carbon monoxide and carbon dioxide concentrations and surface to air exchanges in a rural area (Québec, Canada), Atmos. Environ., 42, 5090–5100, 2008.

Constant, P., Poissant, L., and Villemur, R.: Tropospheric H_2 budget and the response of its soil uptake under the changing environment, Sci. Total Environ., 407, 1809–1823, 2009.

Ehhalt, D. H. and Rohrer, F.: The tropospheric cycle of H_2: a critical review, Tellus B, 61, 500–535, 2009.

Ehhalt, D. H., Schmidt, U., and Heidt, L. E.: Vertical Profiles of Molecular Hydrogen in the Troposphere and Stratosphere, J. Geophys. Res., 82, 5907–5911, 1977.

Fabian, P., Borchers, R., Weiler, K. H., Schmidt, U., Volz, A., Ehhalt, D. H., Seiler, W., and Müller, F.: Simultaneously Measured Vertical Profiles of H_2, CH_4, CO, N_2O, $CFCl_3$, and CF_2Cl_2 in the Mid-Latitude Stratosphere and Troposphere, J. Geophys. Res., 84, 3149–3154, doi:10.1029/JC084iC06p03149, 1979.

Glueckauf, E. and Kitt, G. P.: The hydrogen content of atmospheric air at ground level, Q. J. Roy. Meteorol. Soc., 83, 522–528, 1957.

Gödde, M., Meuser, K., and Conrad, R.: Hydrogen consumption and carbon monoxide production in soils with different properties, Biology And Fertility Of Soils, 32, 129–134, 2000.

Grant, A., Stanley, K. F., Henshaw, S. J., Shallcross, D. E., and O'Doherty, S.: High-frequency urban measurements of molecular hydrogen and carbon monoxide in the United Kingdom, Atmos. Chem. Phys., 10, 4715–4724, doi:10.5194/acp-10-4715-2010, 2010a.

Grant, A., Witham, C. S., Simmonds, P. G., Manning, A. J., and O'Doherty, S.: A 15 year record of high-frequency, in situ measurements of hydrogen at Mace Head, Ireland, Atmos. Chem.

Phys., 10, 1203–1214, doi:10.5194/acp-10-1203-2010, 2010b.

Guo, R. and Conrad, R.: Extraction and characterization of soil hydrogenases oxidizing atmospheric hydrogen, Soil Biol. Biochem., 40, 1149–1154, 2008.

Hammer, S. and Levin, I.: Seasonal variation of the molecular hydrogen uptake by soils inferred from continuous atmospheric observations in Heidelberg, southwest Germany, Tellus B, 61, 556–565, 2009.

Hammer, S., Vogel, F., Kaul, M., and Levin, I.: The H_2/CO ratio of emissions from combustion sources: comparison of top-down with bottom-up measurements in southwest Germany, Tellus B, 61, 547–555, 2009.

Harris, S. H., Smith, R. L., and Suflita, J. M.: In situ hydrogen consumption kinetics as an indicator of subsurface microbial activity, FEMS Microbiology Ecology, 60, 220–228, 2007.

Hauglustaine, D. A. and Ehhalt, D. H.: A three-dimensional model of molecular hydrogen in the troposphere, J. Geophys. Res.-Atmos., 107, 4330, doi:10.1029/2001JD001156, 2002.

Henne, S., Brunner, D., Folini, D., Solberg, S., Klausen, J., and Buchmann, B.: Assessment of parameters describing representativeness of air quality in-situ measurement sites, Atmos. Chem. Phys., 10, 3561–3581, doi:10.5194/acp-10-3561-2010, 2010.

Hurst, D. F., Bakwin, P. S., Myers, R. C., and Elkins, J. W.: Behavior of trace gas mixing ratios on a very tall tower in North Carolina, J. Geophys. Res., 102(D7), 8825–8835, 1997.

Jordan, A. and Steinberg, B.: Calibration of atmospheric hydrogen measurements, Atmos. Meas. Tech., 4, 509–521, doi:10.5194/amt-4-509-2011, 2011.

Khalil, M. A. K. and Rasmussen, R. A.: Global increase of atmospheric molecular hydrogen, Nature, 347, 743–745, 1990.

King, G. M.: Uptake of Carbon Monoxide and Hydrogen at Environmentally Relevant Concentrations by Mycobacteria, Appl. Environ. Microbiol., 69, 7266–7272, doi:10.1128/aem.69.12.7266-7272.2003, 2003a.

King, G. M.: Contributions of Atmospheric CO and Hydrogen Uptake to Microbial Dynamics on Recent Hawaiian Volcanic Deposits, Appl. Environ. Microbiol., 69, 4067–4075, doi:10.1128/aem.69.7.4067-4075.2003, 2003b.

Lallo, M., Aalto, T., Laurila, T., and Hatakka, J.: Seasonal variations in hydrogen deposition to boreal forest soil in southern Finland, Geophys. Res. Lett., 35, L04402, doi:10.1029/2007GL032357, 2008.

Lallo, M., Aalto, T., Hatakka, J., and Laurila, T.: Hydrogen soil deposition at an urban site in Finland, Atmos. Chem. Phys., 9, 8559–8571, doi:10.5194/acp-9-8559-2009, 2009a.

Lallo, M., Aalto, T., Laurila, T., and Hatakka, J.: Hydrogen soil deposition in northern boreal zone, Boreal Environ. Res, 14, 784–793, 2009b.

Langenfelds, R., Francey, R., Pak, B. C., Steele, L. P., Lloyd, J., Trudinger, C. M., and Allison, C. E.: Interannual growth rate variations of atmospheric CO_2 and its $\delta^{13}C$, H_2, CH_4, and CO between 1992 and 1999 linked to biomass burning, Global Biogeochem. Cy., 16, 1048, doi:10.1029/2001GB001466, 2002.

Levin, I.: Atmosphaerisches CO_2, Quellen und Senken auf dem Europaeischen Kontinent, PhD, University of Heidelberg, Heidelberg, Germany, 1984.

Levin, I., Glatzel-Mattheier, H., Marik, T., Cuntz, M., Schmidt, M., and Worthy, D. E.: Verification of German methane emission inventories and their recent changes based on atmospheric obser-

vations, J. Geophys. Res., 104, 3447–3456, 1999.

Liebl, K. H. and Seiler, W.: CO and H_2 destruction at the soil surface, in: Microbial Production and Utilization of Gases, edited by: Schlegel, H. G., Gottschalk, G., and Pfennig, N., Goltze, Göttingen, 215–229, 1976.

Messager, C., Schmidt, M., Ramonet, M., Bousquet, P., Simmonds, P., Manning, A., Kazan, V., Spain, G., Jennings, S. G., and Ciais, P.: Ten years of CO_2, CH_4, CO and N_2O fluxes over Western Europe inferred from atmospheric measurements at Mace Head, Ireland, Atmos. Chem. Phys. Discuss., 8, 1191–1237, doi:10.5194/acpd-8-1191-2008, 2008.

Moxley, J. M. and Cape, J. N.: Depletion of carbon monoxide from the nocturnal boundary layer, Atmos. Environ., 31, 1147–1155, 1997.

Neubert, R. E. M., Spijkervet, L. L., Schut, J. K., Been, H. A., and Meijer, H. A. J.: A computer-controlled continuous air drying and flask sampling system, J. Atmos. Ocean. Tech., 21, 651–659, doi:10.1175/1520-0426(2004)021<0651:ACCADA>2.0.CO;2, 2004.

Novelli, P. C., Lang, P. M., Masarie, K. A., Hurst, D. F., Myers, R., and Elkins, J. W.: Molecular hydrogen in the troposphere: Global distribution and budget, J. Geophys. Res., 104, 30427–30444, 1999.

Pieterse, G., Krol, M. C., Batenburg, A. M., Steele, L. P., Krummel, P. B., Langenfelds, R. L., and Röckmann, T.: Global modelling of H_2 mixing ratios and isotopic compositions with the TM5 model, Atmos. Chem. Phys. Discuss., 11, 5811–5866, doi:10.5194/acpd-11-5811-2011, 2011.

Pison, I., Bousquet, P., Chevallier, F., Szopa, S., and Hauglustaine, D.: Multi-species inversion of CH_4, CO and H_2 emissions from surface measurements, Atmos. Chem. Phys., 9, 5281–5297, doi:10.5194/acp-9-5281-2009, 2009.

Prather, M. J.: An Environmental Experiment with H_2?, Science, 302, 581–582, doi:10.1126/science.1091060, 2003.

Price, H., Jaeglé, L., Rice, A., Quay, P., Novelli, P. C., and Gammon, R.: Global budget of molecular hydrogen and its deuterium content: Constraints from ground station, cruise, and aircraft observations, J. Geophys. Res.-Atmos., 112, D22108, doi:10.1029/2006JD008152, 2007.

Rhee, T. S., Brenninkmeijer, C. A. M., and Röckmann, T.: The overwhelming role of soils in the global atmospheric hydrogen cycle, Atmos. Chem. Phys., 6, 1611–1625, doi:10.5194/acp-6-1611-2006, 2006.

Rice, A., Quay, P., Stutsman, J., Gammon, R., Price, H., and Jaegle, L.: Meridional distribution of molecular hydrogen and its deuterium content in the atmosphere, J. Geophys. Res., 115, D12306, doi:10.1029/2009JD012529, 2010.

Sanderson, M. G., Collins, W. J., Derwent, R. G., and Johnson, C. E.: Simulation of Global Hydrogen Levels Using a Lagrangian Three-Dimensional Model, J. Atmos. Chem., 46, 15–28, 2003.

Schmidt, M., Glatzel-Mattheier, H., Sartorius, H., Worthy, D. E., and Levin, I.: Western European N_2O emissions - A top-down approach based on atmospheric observations, J. Geophys. Res., 106, 5507–5516, 2001.

Schmidt, M., Graul, R., Sartorius, H., and Levin, I.: The Schauinsland CO_2 record: 30 years of continental observations and their implications for the variability of the European CO_2 budget, J. Geophys. Res, 108, 4619, doi:10.1029/2002JD003085, 2003.

Schmitt, S., Hanselmann, A., Wollschläger, U., Hammer, S., and

Levin, I.: Investigation of parameters controlling the soil sink of atmospheric molecular hydrogen, Tellus B, 61, 416–423, 2009.

Schmidt, U.: Molecular hydrogen in the atmosphere, Tellus, 26, 78–90, 1974.

Schmidt, U.: The latitudinal and vertical distribution of molecular hydrogen in the troposphere, J. Geophys. Res., 83, 941–946, 1978.

Schuler, S. and Conrad, R.: Hydrogen oxidation activities in soil as influenced by pH, temperature, moisture, and season, Biology and Fertility of Soils, 12, 127–130, 1991.

Schultz, M. G., Diehl, T., Brasseur, G. P., and Zittel, W.: Air Pollution and Climate-Forcing Impacts of a Global Hydrogen Economy, Science, 302, 624–627, doi:10.1126/science.1089527, 2003.

Scranton, M. I., Barger, W. R., and Herr, F. L.: Molecular hydrogen in the urban troposphere- Measurement of seasonal variability, J. Geophys. Res., 85, 5575–5580, 1980.

Seiler, W., Müller, F., and Oeser, H.: Vertical distribution of chlorofluoromethanes in the upper troposphere and lower stratosphere, Pure and Applied Geophysics, 116, 554–566, 1978.

Simmonds, P. G., Derwent, R. G., O'Doherty, S., Ryall, D. B., Steele, L. P., Langenfelds, R. L., Salameh, P., Wang, H. J., Dimmer, C. H., and Hudson, L. E.: Continuous high-frequency observations of hydrogen at the Mace Head baseline atmospheric monitoring station over the 1994–1998 period, J. Geophys. Res., 105, 12105–12122, 2000.

Smith-Downey, N. V., Randerson, J. T., and Eiler, J. M.: Temperature and moisture dependence of soil H_2 uptake measured in the laboratory, Geophys. Res. Lett., 33, L14813, doi:10.1029/2006GL026749, 2006.

Steinbacher, M., Fischer, A., Vollmer, M. K., Buchmann, B., Reimann, S., and Hueglin, C.: Perennial observations of molecular hydrogen (H_2) at a suburban site in Switzerland, Atmos. Environ., 41, 2111–2124, 2007.

Szegvary, T.: European ^{222}Rn flux map for atmospheric tracer applications, Ph.D. Thesis, Institute of Environmental Geosciences, University of Basel, Switzerland, Basel, 2007a.

Szegvary, T., Leuenberger, M. C., and Conen, F.: Predicting terrestrial ^{222}Rn flux using gamma dose rate as a proxy, Atmos. Chem. Phys., 7, 2789–2795, doi:10.5194/acp-7-2789-2007, 2007b.

Tromp, T. K., Shia, R. L., Allen, M., Eiler, J. M., and Yung, Y. L.: Potential environmental impact of a hydrogen economy on the stratosphere, Science, 300, 1740–1742, 2003.

Vermeulen, A. T., Eisma, R., Hensen, A., and Slanina, J.: Transport model calculations of NW-European methane emissions, Environ. Sci. Policy, 2, 315–324, 1999.

Vermeulen, A. T., Hensen, A., Popa, M. E., van den Bulk, W. C. M., and Jongejan, P. A. C.: Greenhouse gas observations from Cabauw Tall Tower (1992–2010), Atmos. Meas. Tech., 4, 617–644, doi:10.5194/amt-4-617-2011, 2011.

Vollmer, M. K., Juergens, N., Steinbacher, M., Reimann, S., Weilenmann, M., and Buchmann, B.: Road vehicle emissions of molecular hydrogen (H_2) from a tunnel study, Atmos. Environ., 41, 8355–8369, 2007.

Vollmer, M. K., Walter, S., Bond, S. W., Soltic, P., and Röckmann, T.: Molecular hydrogen (H_2) emissions and their isotopic signatures (H/D) from a motor vehicle: implications on atmospheric H_2, Atmos. Chem. Phys., 10, 5707–5718, doi:10.5194/acp-10-5707-2010, 2010.

Warwick, N. J., Bekki, S., Nisbet, E. G., and Pyle, J. A.: Impact of a hydrogen economy on the stratosphere and troposphere studied in a 2-D model, Geophys. Res. Lett., 31, L05107, doi:10.1029/2003GL019224, 2004.

Whittlestone, S. and Zahorowski, W.: Baseline radon detectors for shipboard use: Development and deployment in the First Aerosol Characterization Experiment (ACE 1), J. Geophys. Res., 103, 16743–16751, 1998.

Wilson, S. R., Dick, A. L., Fraser, P. J., and Whittlestone, S.: Nitrous oxide flux estimates for south-eastern Australia, J. Atmos. Chem., 26, 169–188, 1997.

Xiao, X., Prinn, R. G., Simmonds, P. G., Steele, L. P., Novelli, P. C., Huang, J., Langenfelds, R. L., O'Doherty, S., Krummel, P. B., Fraser, P. J., Porter, L. W., Weiss, R. F., Salameh, P., and Wang, R. H. J.: Optimal estimation of the soil uptake rate of molecular hydrogen from the Advanced Global Atmospheric Gases Experiment and other measurements, J. Geophys. Res.-Atmos., 112, D07303, doi:10.1029/2006JD007241, 2007.

Yonemura, S., Kawashima, S., and Tsuruta, H.: Continuous measurements of CO and H_2 deposition velocities onto an andisol: uptake control by soil moisture, Tellus B, 51, 688–700, 1999.

Yonemura, S., Yokozawa, M., Kawashima, S., and Tsuruta, H.: Model analysis of the influence of gas diffusivity in soil on CO and H_2 uptake, Tellus B, 52, 919–933, 2000.

York, D., Evensen, N. M., Martinez, M. L., and Delgado, J. D. B.: Unified equations for the slope, intercept, and standard errors of the best straight line, American Journal of Physics, 72, 367–375, 2004.

Yver, C., Schmidt, M., Bousquet, P., Zahorowski, W., and Ramonet, M.: Estimation of the molecular hydrogen soil uptake and traffic emissions at a suburban site near Paris through hydrogen, carbon monoxide, and radon-222 semicontinuous measurements, J. Geophys. Res., 114, D18304, doi:10.1029/2009JD012122, 2009.

Yver, C. E., Pison, I. C., Fortems-Cheiney, A., Schmidt, M., Chevallier, F., Ramonet, M., Jordan, A., Søvde, O. A., Engel, A., Fisher, R. E., Lowry, D., Nisbet, E. G., Levin, I., Hammer, S., Necki, J., Bartyzel, J., Reimann, S., Vollmer, M. K., Steinbacher, M., Aalto, T., Maione, M., Arduini, J., O'Doherty, S., Grant, A., Sturges, W. T., Forster, G. L., Lunder, C. R., Privalov, V., Paramonova, N., Werner, A., and Bousquet, P.: A new estimation of the recent tropospheric molecular hydrogen budget using atmospheric observations and variational inversion, Atmos. Chem. Phys., 11, 3375–3392, doi:10.5194/acp-11-3375-2011, 2011.